Talanta 219 (2020) 121336

Contents lists available at ScienceDirect

Talanta

journal homepage: www.elsevier.com/locate/talanta

Cannabinoidomics – An analytical approach to understand the effect of medical *Cannabis* treatment on the endocannabinoid metabolome

Paula Berman [a,1], Liron Sulimani [b,c,1], Anat Gelfand [a], Keren Amsalem [a], Gil M. Lewitus [a], David Meiri [a,*]

[a] The Laboratory of Cancer Biology and Cannabinoid Research, Department of Biology, Technion-Israel Institute of Technology, Haifa, 3200003, Israel
[b] The Kleifeld Laboratory, Department of Biology, Technion-Israel Institute of Technology, Haifa, 3200003, Israel
[c] Cannasoul Analytics, Caesarea, Israel

ARTICLE INFO

Keywords:
Phytocannabinoids
Endocannabinoids
Cannabis sativa L.
Cannabidiol
LC/HRMS
Mass spectral library

ABSTRACT

Increasing evidence for the therapeutic potential of *Cannabis* in numerous pathological and physiological conditions has led to a surge of studies investigating the active compounds in different chemovars and their mechanisms of action, as well as their efficacy and safety. The biological effects of *Cannabis* have been attributed to phytocannabinoid modulation of the endocannabinoid system. *In-vitro* and *in-vivo* studies have shown that pure phytocannabinoids can alter the levels of endocannabinoids and other cannabimimetic lipids. However, it is not yet understood whether whole *Cannabis* extracts exert variable effects on the endocannabinoid metabolome, and whether these effects vary between tissues. To address these challenges, we have developed and validated a novel analytical approach, termed "cannabinoidomics," for the simultaneous extraction and analysis of both endogenous and plant cannabinoids from different biological matrices. In the methodological development liquid chromatography high resolution tandem mass spectrometry (LC/HRMS/MS) was used to identify 57 phytocannabinoids, 15 major phytocannabinoid metabolites, and 78 endocannabinoids and cannabimimetic lipids in different biological matrices, most of which have no analytical standards. In the validation process, spiked cannabinoids were quantified with acceptable selectivity, repeatability, reproducibility, sensitivity, and accuracy. The power of this analytical method is demonstrated by analysis of serum and four different sections of mouse brains challenged with three different cannabidiol (CBD)-rich extracts. The results demonstrate that variations in the minor phytocannabinoid contents of the different extracts may lead to varied effects on endocannabinoid concentrations, and on the CBD metabolite profile in the peripheral and central systems. We also show that the *Cannabis* challenge significantly decreases the levels of several endocannabinoids in specific brain sections compared to the control group. This effect is extract-specific and suggests the importance of minor, other-than CBD, phytocannabinoid or non-phytocannabinoid compounds.

Abbreviations: 11-COOH-gluc-THC, 11-nor-9-carboxy-Δ^9-THC glucuronide; 11-COOH-THC, 11-nor-carboxy-Δ^9-*trans*-tetrahydrocannabinol; 11-OH-THC, 11-hydroxy-Δ^9-*trans*-tetrahydrocannabinol; 12-LOX, 12-lipoxygenase; 15-LOX, 15-lipoxygenase; 2-AG, 2-arachidonoylglycerol; AA, arachidonic acid; AcOH, acetic acid; AEA, anandamide; AGC, automatic gain control; CB1, cannabinoid receptor type 1; CB2, cannabinoid receptor type 2; CBC, cannabichromene; CBCA, cannabichromenic acid; CBCV, cannabichromevarin; CBD, cannabidiol; CBDA, cannabidiolic acid; CBDV, cannabidivarin; CBDVA, cannabidivarinic acid; CBG, cannabigerol; CBGA, cannabigerolic acid; CBG-C4, cannabigerol-C4; CBL, cannabicyclol; CBN, cannabinol; CBNA, cannabinolic acid; CNS, central nervous system; COX-2, cyclooxygenase-2; CYP, cytochrome P450; DAGL, diacylglycerol lipase; DHA, docosahexaenoic acid; d-IS, deuterated internal standard; eCBs, endocannabinoids and other endogenous cannabimimetic lipids; eCBS, endocannabinoid system; EPA, eicosapentaenoic acid; FA, fatty acid; FAAH, fatty acid amide hydrolase; GPCR, G-protein-coupled receptor; HPLC, high performance liquid chromatography; HSD, honest significant difference; IT, injection time; LA, linoleic acid; LC/HRMS, liquid chromatography high-resolution mass spectrometry; LC/MS, liquid chromatography mass spectrometry; LnA, linolenic acid; LOQ, limit of quantification; MAG, 2-monoacyl glycerol; MAGL, monoacyl-glycerol lipase; MS-dd-MS^2, full MS^1 followed by data dependent MS/MS; NAPE-PLD, N-acyl-phosphatidyl-ethanolamine-selective phospho-lipase D; N-EA, N-acyl ethanolamide; N-Gly, N-acyl glycine; OA, oleic acid; PA, palmitic acid; PRM, parallel reaction monitoring; PUFA, polyunsaturated fatty acid; RSD, relative standard deviation; RT, retention time; SA, stearic acid; SPE, solid phase extraction; UHPLC, ultra HPLC; Δ^8-THC, (−)-Δ^8-*trans*-tetrahydrocannabinol; Δ^9-THC, (−)-Δ^9-*trans*-tetrahydrocannabinol; Δ^9-THCA, (−)-Δ^9-*trans*-tetrahydrocannabinolic acid; Δ^9-THC-C4, (−)-Δ^9-*trans*-tetrahydrocannabinol-C4; Δ^9-THCO, (−)-Δ^9-*trans*-tetrahydrocannabiorcol-C1; Δ^9-THCV, (−)-Δ^9-*trans*-tetrahydrocannabivarin.

* Corresponding author. Technion-Israel Institute of Technology, Haifa, 3200003, Israel.
E-mail address: dmeiri@technion.ac.il (D. Meiri).

[1] The authors contributed equally to this publication.

https://doi.org/10.1016/j.talanta.2020.121336
Received 21 May 2020; Received in revised form 24 June 2020; Accepted 25 June 2020
Available online 10 July 2020

1. Introduction

Phytocannabinoids are found almost uniquely in *Cannabis sativa* L. (*Cannabis*). Many of the pharmacological and therapeutic properties of phytocannabinoids rely on their interactions with the endocannabinoid system (eCBS), present in animals and humans. This interaction makes *Cannabis* treatment especially valuable since eCBS modulation has been suggested as an emerging target of pharmacotherapy, with therapeutic potential in almost all diseases affecting humans [1]. Up until the last decade, the eCBS was defined as the ensemble of (i) two G-protein-coupled receptors (GPCR), cannabinoid receptors type 1 and 2 (CB1 and CB2, respectively); (ii) their two most studied endogenous ligands, the endocannabinoids N-arachidonoylethanolamide (AEA) and 2-arachidonoylglycerol (2-AG); and (iii) the enzymes responsible for endocannabinoid biosynthesis [i.e., *N*-acyl-phosphatidyl-ethanolamine -selective phospholipase D (NAPE-PLD) and diacylglycerol lipase (DAGL) for AEA and 2-AG, respectively] and hydrolytic inactivation [i.e., fatty acid amide hydrolase (FAAH) and monoacylglycerol lipase (MAGL), for AEA and 2-AG, respectively] [2–4]. More recently, additional receptors, biosynthesizing and degrading enzymes, endocannabinoids and other cannabimimetic lipids have been recognized as part of an extended eCBS [2,5–7] or an "endocannabinoidome" [2].

It has been suggested that phytocannabinoids can act upon the extended eCBS directly, activating and/or inhibiting cannabinoid and non-cannabinoid receptors such as the thermosensitive transient receptor potential cation channels, several orphan GPCR receptors, and peroxisome proliferator-activated nuclear receptors, and/or indirectly, by modulating the amount of available endocannabinoids [2,5–7]. This modulation can result from phytocannabinoid inhibition of the metabolizing enzymes, intracellular transporters and more [2].

Isolating the pharmacological effects of *Cannabis* extracts is complex given that more than 150 different phytocannabinoids have been identified in *Cannabis* chemovars [8–10], with widely varying concentrations between chemovars [10]. An additional complexity is that *Cannabis* may be consumed via different routes (inhalation, oral, ophthalmic, rectal, sublingual or dermal administration), each with different pharmacokinetic behaviors, leading to differential tissue and body fluid distributions over time [11–13]. Finally, phytocannabinoids are endogenously metabolized, mainly in the liver, by enzymes of the cytochrome P450 (CYP) complex [12], producing metabolites that can have pharmacological and biological roles of their own. The existence and concentration of the different metabolites also differs between mammalian species, due to variations in their available metabolizing enzymes [12,14].

Another complexity in phytocannabinoid pharmacology is that one compound may simultaneously act upon different receptors and/or enzymes [2,15]. This naturally becomes even more challenging to identify or describe in the case of whole *Cannabis* treatment, which consists of tens of phytocannabinoid components at varying concentrations, leading to polypharmacological effects on the extended eCBS. This often leads to different phytocannabinoids competing for the same receptors or affecting the binding affinity of other compounds [15–17]. Isolating the effect of specific phytocannabinoid compositions from specific *Cannabis* chemovars is crucial for elucidating mechanisms of action and ultimately harnessing and tailoring the potential of *Cannabis* therapeutics. To this end, chemical analysis methods are essential to quantitatively analyze endocannabinoids, phytocannabinoids and their metabolites in biological matrices.

Endocannabinoid metabolites are all derivatives of long chain fatty acids (FAs) and are classified according to the lipid class to which they belong. Compounds belonging to more than 20 different lipid classes have been suggested to interact with the extended eCBS, making this group of metabolites extremely diverse [6,18–23]. Several liquid chromatography mass spectrometry (LC/MS) methods for analyzing specific lipid classes from different biological samples have been reported and are summarized in a number of recent reviews [19–22]. Several of these methods use a lipidomic approach for the simultaneous profiling of tens of lipids from different groups.

LC/MS methods for quantification of phytocannabinoids and their metabolites in biological matrices have also been developed and were recently reviewed by Abd-Elsalam et al. [24]. The vast majority of studies analyze only the three best known phytocannabinoids, (−)-Δ^9-*trans*-tetrahydrocannabinol (Δ^9-THC), cannabidiol (CBD), cannabinol (CBN); and the three major Δ^9-THC metabolites, 11-hydroxy-Δ^9-*trans*-tetrahydrocannabinol (11-OH-THC), 11-nor-carboxy-Δ^9-*trans*-tetrahydrocannabinol (11-COOH-THC), and 11-nor-9--carboxy-Δ^9-THC glucuronide (11-COOH-gluc-THC), none of CBD. While a few studies have also included (−)-Δ^9-*trans*-tetrahydrocannabinolic acid (Δ^9-THCA), cannabigerol (CBG), cannabichromene (CBC), cannabidivarin (CBDV) and (−)-Δ^9-*trans*-tetrahydrocannabivarin (Δ^9-THCV) [25–28], they still only present a very narrow view of the rich phytocannabinoid profile of whole *Cannabis* therapeutics.

In this study, we therefore describe a novel "cannabinoidomic" (endocannabinoid and phytocannabinoid "omic") method for simultaneous extraction, identification and quantification of endocannabinoids and other endogenous cannabimimetic lipids (collectively designated in this study as eCBs), phytocannabinoids, and several of their metabolites, in various biological matrices, via liquid chromatography high-resolution mass spectrometry (LC/HRMS). A single extraction method is especially important in clinical and pre-clinical studies, which often have limited sample sizes. To the best of our knowledge, this is the first time that such a comprehensive method has been developed and validated. We also demonstrate the importance and power of this method by analyzing changes in concentrations of eCBs in serum and four different brain sections, following their challenge with three different CBD-rich whole plant extracts.

2. Materials and methods

2.1. Reagents and materials

LC/MS grade acetonitrile, methanol, and water for the mobile phase, and high performance liquid chromatography (HPLC) grade acetonitrile, methanol, water and ethanol for sample preparation were obtained from Mercury Scientific and Industrial Products Ltd. (Rosh Haayin, Israel). LC/MS grade acetic acid (AcOH) and serum (S1-100 mL) for method validation were purchased from Sigma-Aldrich (Rehovot, Israel). A list of all the analytical (>98%) and deuterated internal standards (d-ISs) appears in Table S1. Air-dried medical *Cannabis* chemovars were obtained from several Israeli medical *Cannabis* distributors.

2.2. Mice

Adult (8–10 weeks of age; 20–25 g) male C57BL/6 mice (C57BL/6J; The Jackson Laboratory) were used in all experiments. All experiments were performed in accordance with the National Institutes of Health's Guide for the Care and Use of Laboratory Animals. All procedures and protocols were approved by the Technion Administrative Panel of Laboratory Animal Care (#:IL_130-11-2015).

2.3. Sample preparation and extraction

Phytocannabinoid extraction from *Cannabis* and their analysis by LC/HRMS were performed according to our previously published methods [10,29]. The full description appears in Method S1. For the *Cannabis* challenge, extracts were reconstituted into a vehicle solution consisting of 1:1:18 ethanol:cremophor:saline into a final concentration of 20 mg mL^{-1}.

For the method development and validation, naïve mice were sacrificed and their blood, brain, liver, spleen and colon tissues were collected, and immediately frozen in liquid nitrogen. Blood samples collected via cardiac puncture were set aside for 30 min at room

temperature and then centrifuged for 30 min at 4 °C. The separated serum and all the other tissues were stored at −80 °C until analysis.

The extraction solution for all samples consisted of methanol: acetonitrile:AcOH in a ratio of 50:50:0.1 v/v, spiked with d-ISs. Whole tissues were rapidly dissected into smaller fractions on dry ice, weighed and homogenized in the extraction solution (brain, liver, spleen and colon tissues were extracted with 6, 10, 8 and 8 mL, respectively) using a beads homogenizer (1600 MiniG, SPEX Sample Prep, Metchen, NJ, US), and shaken in an orbital shaker for 30 min. Volumes of 200 μL serum were thoroughly vortexed with 600 μL of the extraction solution. All samples were then centrifuged at 14,000 rpm, 4 °C for 20 min. Volumes of 1 and 0.8 mL were collected from the tissues and serum supernatants, respectively, diluted with 3 mL 0.1% v/v AcOH in water, and loaded onto pre-conditioned Agela Cleanert C8 solid phase extraction (SPE) cartridges (500 mg of sorbent, 50 μm particle size). Whole cannabinoids were eluted from the SPE columns with 2 mL 0.1% v/v AcOH in methanol, evaporated to dryness by SpeedVac, reconstituted in 100 μL ethanol and filtered through a 0.22 μm PTFE syringe filter for LC/HRMS analysis.

2.4. LC/HRMS chemical analysis

LC/HRMS analyses were performed using a Thermo Scientific ultra HPLC (UHPLC) system coupled with a Q Exactive™ Focus Hybrid Quadrupole-Orbitrap MS (Thermo Scientific, Bremen, Germany). The chromatographic separation was achieved using a Halo C18 Fused Core column (2.7 μm, 150 mm × 2.1 mm i.d.) with a guard column (2.7 μm, 5 mm × 2.1 mm i.d) (Advanced Materials Technology, Delaware, USA) and a ternary A/B/C multistep gradient (solvent A: 0.1% AcOH in water, solvent B: 0.1% AcOH in acetonitrile, and solvent C: methanol). The multistep gradient program was set as follows: initial conditions were 50% B raised to 67% B until 3 min, held at 67% B for 5 min, and then raised to 90% B until 12 min, held at 90% B until 15 min, decreased to 50% B over the next min, and held at 50% B until 20 min for re-equilibration of the system prior to the next injection. Solvent C was initially 5% and then lowered to 3% until 3 min, held at 3% until 8 min, raised to 5% until 12 min and then kept constant at 5% throughout the run. A flow rate of 0.25 mL min^{-1} was used, the column temperature was 30 °C and the injection volume was 1 μL.

MS acquisition was carried out with a heated electro spray ionization ion source operated in switching mode. The source parameters were similar for both negative and positive modes: sheath gas flow rate, auxiliary gas flow rate and sweep gas flow rate: 50, 20 and 0 arbitrary units respectively; capillary temperature: 350 °C; heater temperature: 50 °C; spray voltage: 3.00 kV.

MS/MS identification of compounds was performed in full MS^1 followed by data dependent MS/MS (MS-dd-MS^2) or parallel reaction monitoring (PRM) modes. Data acquisition in full MS^1 mode was performed at 70,000 resolution, the scan range was 150–750 *m/z* and the automatic gain control (AGC) target was set to 10^6 with a maximum injection time (IT) of 100 ms. Data acquisition in dd-MS^2 or PRM modes were performed at 17,500 resolution, the AGC target was set to 10^5 with a maximum IT of 50 ms and an isolation window of 2 *m/z*.

Quantification of whole cannabinoids was performed in full MS^1 mode. Ten point standard mixes of the available analytical standards were prepared in ethanol and spiked with a mixture of all d-ISs at a final concentration of 15 ng mL^{-1}. Final calibration ranges were as follows: 0.1–1000 ng mL^{-1} for all compounds excluding Δ^9-THCV, cannabicyclol (CBL) and cannabicitran, which were added in the range of 0.05–500 ng mL^{-1}, and CBC, CBDV, CBG, CBN, cannabidivarinic acid (CBDVA), cannabigerolic acid (CBGA), cannabichromevarin (CBCV), cannabichromenic acid (CBCA), cannabinolic acid (CBNA), and Δ^8-*trans*-tetrahydrocannabinol (Δ^8-THC), which were prepared in the range of 0.025–250 ng mL^{-1} each.

2.5. Method validation

The method was validated only for the compounds with analytical standards. Calibration curves were determined empirically according to the weighted least-squares linear regression method with a weighting factor of 1/X. Limits of quantification (LOQs) were determined as the lowest point in the calibration curve for which maximum deviation from expected concentrations of 20% was observed, and minimum signal-to-noise ratios of 10. All the standard mixes were stored at −20 °C in amber vials. Selectivity of phytocannabinoids in biological matrices was determined by screening of phytocannabinoids in blank matrices according to retention time (RT) and accurate mass. Since eCBs exist in non-spiked biological matrices, the selectivity for these compounds was determined by spiking biological matrices with a mix of the standard compounds, and comparing the MS/MS spectra of each component to that of the ethanol standard mix. Resolution was calculated for adjacent compounds with the same accurate mass. Acceptable values for the resolution were considered to be ≥ 1.5.

Accuracy and precision were determined by spiking each biological matrix with two concentration levels of the standard mixes on three different days. For the validation of serum samples, 200 μL of commercial human serum was spiked in triplicates with 600 μL of the extraction solution, consisting of different concentrations of the standard mix and d-ISs. For the validation of tissues, dissected samples were cut into smaller segments and homogenized in the extraction solution. The homogenate was then divided into several fractions and standards at two different concentrations and d-ISs were added to each fraction. Each concentration was prepared in duplicates.

Accuracy was determined to be the percent difference between the mean concentration of the spiked analyses in relation to the non-spiked and expected concentrations. The precision of the whole method was assessed by calculating the relative standard deviations (RSDs) for repeatability and reproducibility of the same spikes. Repeatability was quantified by intra-day variation by analyzing three samples from the same tissue on the same day ($n = 3$); and reproducibility was quantified by inter-day variation, analyzing the same sample in triplicate on three different days ($n = 9$).

2.6. Study of the effect of three equally high CBD Cannabis extracts on the eCB metabolome in serum and different brain parts

Saline or three equally high-CBD *Cannabis* extracts (50% w/w) were injected intraperitoneally (150 mg kg^{-1}). Mice were sacrificed 30 min post-injection, and their brains and blood were immediately collected and treated as described in the method development (section 2.3). Brains were dissected on an ice-cold dissection plate into the following regions: cortex, cerebellum, hippocampus and hypothalamus. The separated parts and serum were immediately frozen in liquid nitrogen, and stored in −80 °C until extraction.

One-way ANOVA was used to determine the statistical significance of five samples. P-values were corrected for multiple testing using the Tukey honest significant difference (HSD) post hoc test (*$p < 0.05$, **$p < 0.01$, ***$p < 0.001$, ****$p < 0.0001$).

3. Results and discussion

3.1. Method development and identification of whole cannabinoids in biological matrices

First, a list of relevant compounds and their masses was compiled based on the available literature. In a previous publication, we established a novel MS/MS spectral library consisting of 94 phytocannabinoids, where, due to the lack of analytical standards (only 13 standards available at that time), most of the compounds were putatively identified in different *Cannabis* extracts [10]. This library includes known phytocannabinoids from all 10 phytocannabinoid subclasses (Fig. 1A)

and some additional unknowns. Since phytocannabinoids are endogenously metabolized in the body, analyzing some of the major types of metabolites previously identified in human and animal blood and tissues was also important for our method, e.g., phytocannabinoids with added hydroxyl, carboxyl, glucuronide or carboxy-glucuronide groups [11–14]. Phytocannabinoids are precursors for an overwhelming number of metabolites that can be potentially produced in the body. Therefore, for practical purposes, we focused only on metabolites of the major phytocannabinoids in decarboxylated extracts, Δ^9-THC and CBD, as shown in Fig. 1B. For the eCBs, compounds from 15 lipid families [6, 18–23] with at least one analytical standard available for each class were considered. In each family, we considered eight potential FA derivatives (Fig. 1C): eicosapentaenoic acid (EPA), linolenic acid (LnA), docosahexaenoic acid (DHA), arachidonic acid (AA), linoleic acid (LA), palmitic acid (PA), oleic acid (OA), and stearic acid (SA). Not all these derivatives have been previously identified in biological samples, however there is a potential for interaction with the extended eCBS, as suggested in the literature [6,19,21,22]. The compiled cannabinoidomic list of masses appears in Table S2. The names of the compounds were abbreviated by the FA derivative and lipid head group.

The LC/HRMS conditions used for data acquisition were determined using a mixture of all the analytical standards prepared in ethanol. For the UHPLC method, we used the chromatographic conditions previously established for comprehensive phytocannabinoid profiling of *Cannabis* extracts [10], with an additional 16 min at the high organic load, in order to allow for the highly lipophilic compounds from the biological matrices (mainly FAs) to elute from the column. In order to identify the adduct ions for each type of molecule, the mix of standards was first analyzed in full MS^1 mode with polarity switching. Phytocannabinoids and their metabolites were best identified in negative mode ($[M-H]^-$) except for cannabicitran, which was identified in positive mode ($[M+H]^+$). Compounds from the different lipid families were identified in either negative or positive modes, according to the observed hydrogen ($[M-H]^-/[M+H]^+$) and/or acetate $[M+CH3COOH]^-$ adducts (Table S2). For 2-monoacyl glycerols (MAGs) and N-acyl ethanolamides (N-EAs), both $[M+CH3COOH]^-$ and $[M+H]^+$ adducts were observed (Table S2), while the acetate form appeared as the major ion.

Optimization of the sample preparation method was performed by spiking a mixture of the available analytical standards and d-ISs into a commercial serum sample, and calculating the extraction recovery. Liquid solvent extraction followed by protein and cells precipitation, SPE, drying, and reconstitution in ethanol, were chosen as the preferred extraction methods for all the biological matrices. Tissues were additionally dissected into smaller fractions and homogenized prior to liquid extraction, in order to increase the overall surface area contact between the extraction solvent and the sample. Protein and cells precipitation and SPE steps were performed in order to reduce matrix effects, contamination of the LC/HRMS instrument and increase sensitivity.

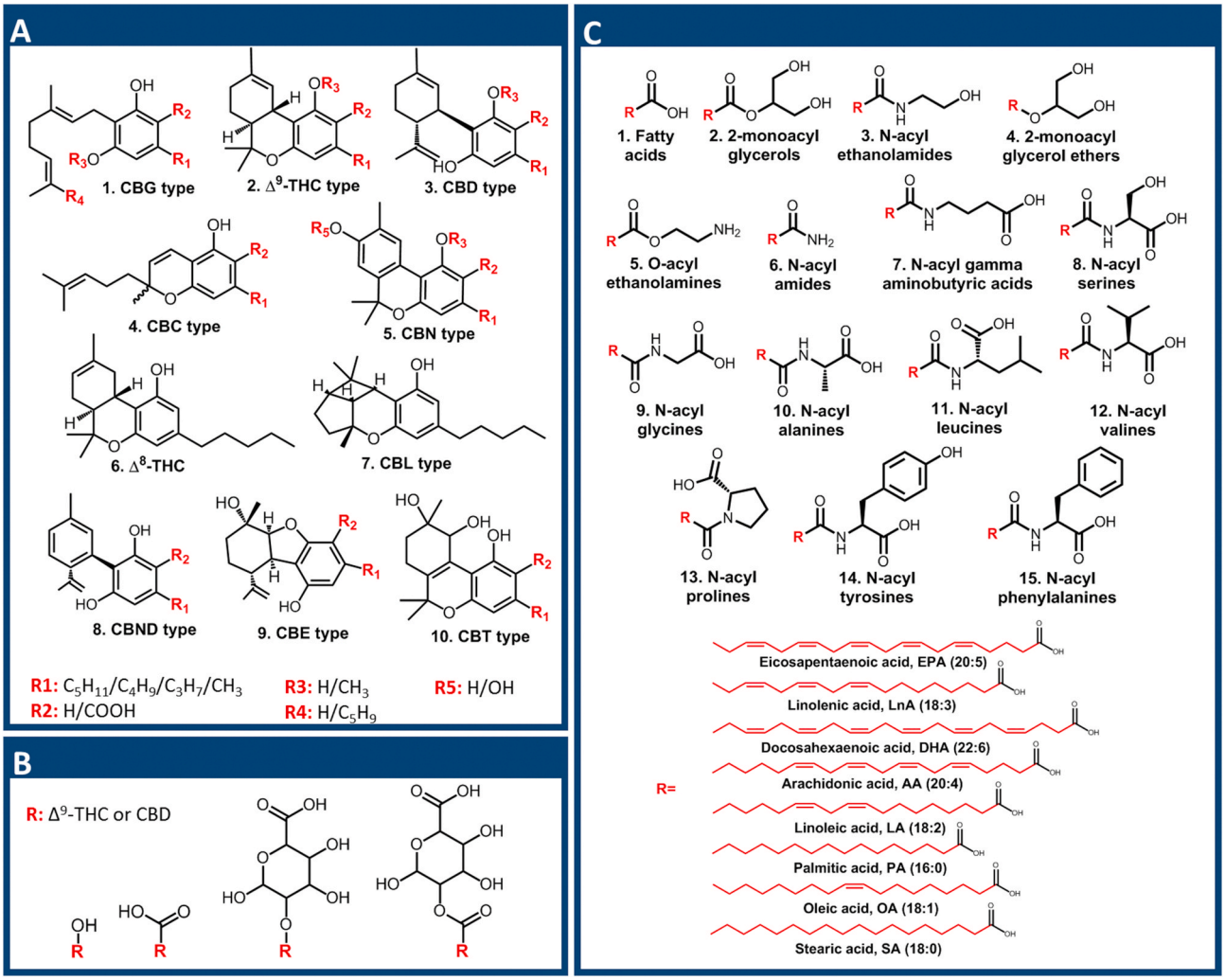

Fig. 1. The cannabinoidomic library of relevant compounds compiled in this research. The library includes: (**A**) Phytocannabinoids from all 10 subclasses as recently identified in different *Cannabis* extracts [10]; (**B**) major Δ^9-THC and CBD metabolites; and (**C**) eCB and cannabimimetic lipids from 15 lipid families, each consisting of 8 potential FA derivatives.

Different solvents, including methanol, acetonitrile, ethanol and hexane, with and without AcOH, were considered for the liquid and SPE extractions. AcOH in either methanol or acetonitrile yielded the highest recoveries for either most of the endogenous lipids or phytocannabinoids, respectively. The extraction solvent therefore, was chosen as a mixture of methanol:acetonitrile:AcOH in the ratio of 50:50:0.1 v/v.

One major obstacle in the development of this method was the lack of analytical standards (the available standards are marked with an asterisk in Table S2), making identification and quantification of many relevant compounds extremely challenging. In order to cope with these challenges, we screened blood and tissues from mice with and without *Cannabis* treatment, in order to identify additional compounds. To this end, the LC/HRMS instrument was operated in MS-dd-MS^2 or PRM modes according to the list of masses in Table S2.

3.1.1. Phytocannabinoids

Identification of additional phytocannabinoids in biological samples, for which there were no analytical standards available, was performed by spectral matching against our developed MS/MS spectral library of phytocannabinoids in *Cannabis* extracts [10]. In order to verify that the identification of the phytocannabinoids in biological matrices is not changed compared to the plant matrix, we spiked commercial serum samples with predominant Δ^9-THC, CBD, Δ^9-THCA or cannabidiolic acid (CBDA) extracts, and analyzed them using the developed method. The RTs and MS/MS spectra for the observed phytocannabinoids in the spiked samples corresponded with those in the extracts and with our MS/MS spectral library [10] (Fig. S1). Several of the phytocannabinoids were observed in the spiked serum samples but not in the extract [for example (−)-Δ^9-*trans*-tetrahydrocannabinol-C4 (Δ^9-THC-C4) and (−)-Δ^9-*trans*-tetrahydrocannabiorcol-C1 (Δ^9-THCO)] due to improved sensitivity following SPE and reconstitution of the serum samples. Minor peaks with the same accurate mass and RT as CBN, cannabigerol-C4 (CBG-C4) and 373-12b appeared in the blank matrix (Fig. S1).

3.1.2. Δ^9-THC and CBD metabolites

Despite the importance of quantifying concentrations of phytocannabinoid metabolites in different tissues, there are currently only three analytical standards of Δ^9-THC metabolites commercially available (11-OH-THC, 11-COOH-THC and 11-COOH-gluc-THC), none of CBD. Therefore, putative identification of major Δ^9-THC and CBD

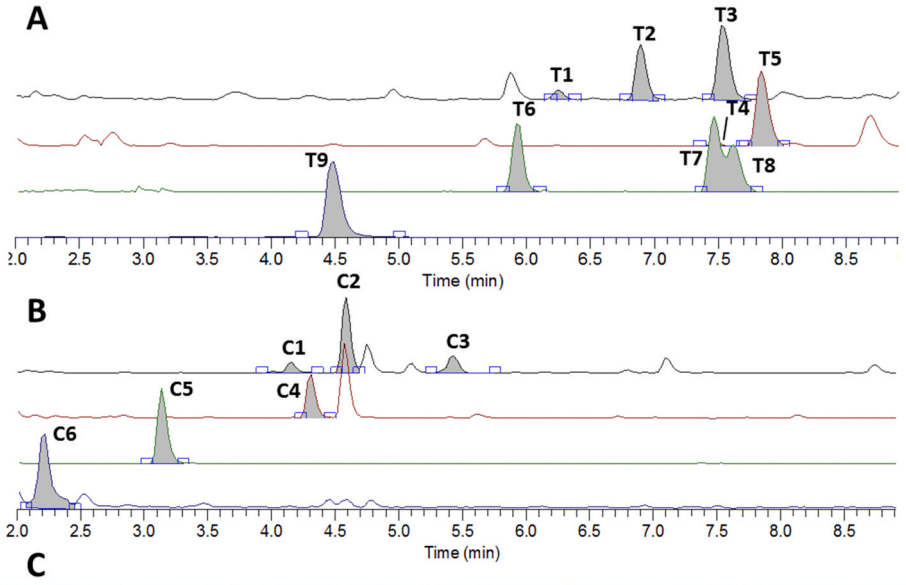

C

Peak	Name	Accurate mass $[M-H]^-$ [Da]	RT [min]	Typical fragments [Da]
T1	OH-THC1	329.2122	6.23	311.201, 173.097
T2	OH-THC2	329.2122	6.89	311.201, 173.097
T3	11-OH-THC[a]	329.2122	7.52	311.201, 173.097
T4	COOH-THC1	343.1915	7.46	325.181, 299.202
T5	11-COOH-THC[a]	343.1915	7.84	325.181, 299.202
T6	THC-glucuronide1	489.2494	5.92	113.025, 85.029
T7	THC-glucuronide2	489.2494	7.47	113.025, 85.029
T8	THC-glucuronide3	489.2494	7.62	113.025, 85.029
T9	11-COOH-glucuronide-THC[a]	519.2236	4.47	113.025, 85.029
C1	OH-CBD1	329.2122	4.20	311.201, 173.097
C2	OH-CBD2	329.2122	4.60	311.201, 173.097
C3	OH-CBD3	329.2122	5.43	311.201, 173.097
C4	COOH-CBD	343.1915	4.31	325.181, 299.202
C5	CBD-glucuronide	489.2494	3.13	113.025, 85.029
C6	COOH-glucuronide-CBD	519.2236	2.22	113.025, 85.029

[a]Absolute identification by analytical standard

Fig. 2. Identification of major phytocannabinoid metabolites by LC/HRMS/MS. Extracted ion chromatograms of the identified (**A**) Δ^9-THC (T1-T9) and (**B**) CBD (C1–C6) metabolites and their (**C**) peak annotations, accurate masses and RTs.

metabolites was performed by screening serum samples from mice sacrificed 0.5 and 24 h post *Cannabis* injection of either Δ^9-THC- or CBD-rich extracts, respectively. Since Δ^9-THC and CBD have the same chemical formula, so do their metabolites. Therefore, metabolites with the same accurate mass were differentiated based upon RT and MS/MS spectra. This data, however, did not provide enough information to clearly elucidate the specific structural isomer for each peak. Phytocannabinoid metabolites were therefore identified by type, according to accurate mass and precursor (T and C for metabolites from Δ^9-THC and CBD, respectively, Fig. 2A–C, and Fig. S2).

The samples were analyzed in MS-dd-MS^2 mode with a normalized collision energy of 40. The accurate masses used for the screen were *m/z* of 329.2122, 343.1915, 489.2494 and 519.2236, which correspond to the addition of hydroxyl, carboxyl, glucuronide and carboxy-glucuronide groups, respectively (Fig. 1B). Since we previously identified the masses corresponding with hydroxylated and carboxylated forms of Δ^9-THC and CBD in *Cannabis* extracts [10], we proceeded to compare the spectra of the identified compounds against those present in the *Cannabis* extract used for the injections, and against our developed library of phytocannabinoids, to exclude any compounds originating from the plant.

As expected from the higher lipophilicity of Δ^9-THC compared to CBD [10], the identified Δ^9-THC metabolites elute later than those originating from CBD with the same functional group (Fig. 2A and B for the identified Δ^9-THC and CBD metabolites, respectively, annotations appear in Fig. 2C). In addition, the same type of Δ^9-THC and CBD metabolites exhibit several product ions with different relative intensities, as previously reported for Δ^9-THC and CBD [10]. Furthermore, the different metabolites have specific fragments consistent with the cleavage of the new functional groups (Fig. S2A–S2C). For example, the hydroxy-, carboxy- and glucuronide-phytocannabinoids display water, CO_2 and glucuronide neutral losses, respectively (Fig. 2C). All these findings, along with the fact that these compounds were not observed in blank serum or *Cannabis* extracts, increase the confidence of the putative identification. Overall, fifteen major Δ^9-THC and CBD metabolites were identified, three of which were verified using analytical standards (T3, T5 and T9, Fig. S2C).

3.1.3. eCBs

As for eCBs, additional compounds from each family, for which there were no standards commercially available, were screened in extracts from different mice tissues. The samples were analyzed in MS-dd-MS^2 or PRM modes. Accurate masses in the MS/MS list of relevant masses were determined according to the polarity and adduct identified for the analytical standard from the same lipid class (Table S2). The acetate form of MAGs and N-EAs was not observed in MS/MS experiments probably due to in-source fragmentation. Therefore, MS/MS analyses for identification of additional compounds from these two groups, were performed according to the $[M+H]^+$ ions.

The additional compounds were putatively identified in different mice tissues according to accurate mass, relative RT and typical MS/MS fragment, as follows: Generally speaking, the relative chromatographic order of elution for the different FA derivatives from all the lipid classes was constant, with a shift for the absolute RT in relation to the head group, as shown in Fig. 3A and B, for the elution of FAs and N-EAs, respectively. Also, the MS/MS spectra of the different N-acyl families, showed a characteristic fragment corresponding to the fragmentation of the head group. For example, the fragment with *m/z* of 62.0601 (Fig. 3C) for all N-EA derivatives, corresponds with the loss of the ethanolamine head group (Fig. 3D). A list of the eCBs putatively identified in this research appears in Table S3. We also searched by the same method for compounds from N-acyl-tryptophan and N-acyl-methionine families, which have been previously identified in the brain [6,30]. However, no potential compounds from these groups were identified in any of the tissues analyzed in this study.

A summary of all the identified compounds, analytical and d-ISs standards in this study appears in Table S4. This cannabinoidomic library of compounds could be further expanded using other biological matrices and *Cannabis* extracts, following the chromatographic and MS characteristics suggested in this research.

3.2. Quantification and method validation

Quantification was performed in full MS^1 mode with polarity switching due to the vast amount of compounds analyzed (Table S2) with many peaks overlaps. The excellent mass resolution achieved in this mode by the Orbitrap mass analyzer (acquisition was performed with a resolution of 70,000) provides improved sensitivity compared to MS/MS acquisitions (since the parent ion is analyzed and not a product ion) for the same instrument. This allows for the reprocessing of previously acquired data in order to pinpoint additional suspect compounds whose concentrations change due to the applied treatment and that may have biological importance.

In order to verify that the concentrations achieved by this mode are accurate and precise, we validated the method for the compounds with analytical standards. All the analyzed standards fell well within the total runtime of this method, with acceptable (>1.5) resolutions (Table S5). In order to determine the selectivity of our method in biological matrices, we spiked a commercial serum sample with a mix of the standard compounds, and compared the extracted ion chromatogram and MS/MS spectra of each component to that of the ethanol standard mix. Since 2-MAGs spontaneously undergo isomerization to biologically inactive 1-MAGs through the migration of the acyl group from sn-2 to sn-1/3 position [18,31,32], in this study, we summed the peaks of 1- and 2-MAGs (total MAGs), as previously suggested in the literature [33,34]. FAs and N-oleoyl amide exhibited background peaks in blank injections. These were however, considerably lower (at least 2 orders of magnitude lower) than the peaks observed in the different biological matrices. For the method validation, we therefore used only the standards of AA and LnA that showed lower concentrations in the different matrices. 1-Palmitoyl glycerol showed pronounced background peaks and was therefore removed from the developed method. A minor peak with the same accurate mass and RT as CBN appeared in the blank matrix, therefore the area of this peak was determined as the LOQ for this compound.

Cannabinoid concentrations were quantified according to the stable isotope dilution method, by which the amount of each compound is corrected in both calibration curves and biological samples according to d-ISs. Since there was only a limited number of d-ISs compared to the number of analytes, we quantified all the members of the same lipid class using the d-IS from each family, as summarized in Table S6. All calibration curves were linear with excellent fits ($R^2 > 0.99$ for all compounds, Table S6) and had less than 20% deviation from expected values in the concentration ranges studied for each compound. Accuracy and precision were determined by spiking serum, brain, liver, colon and spleen samples with two different concentration levels of the standard mixes (5 and 50 ng mL^{-1}) on different days as presented in Tables S7A and S7B, respectively. For the vast majority of the cannabinoids with d-ISs, acceptable accuracy and precision values were observed in the two concentrations and for all five matrices (90–110% and RSDs<15%, respectively). Most other cannabinoids were identified with acceptable accuracies within the range of 80–120%, and had less than 15% repeatability and reproducibility values. Several other compounds showed lower values, probably due to a less suitable d-IS, which does not correct for matrix and/or recovery. Still these compounds can be differentially quantified to observe changes in concentrations in relation to a specific treatment, disease or condition. Δ^8-THC and CBL showed consistently low recoveries and were therefore removed from the developed method.

A limitation of this method relates to several additional groups with analytical standards, also associated with the extended eCBS, that have been identified and characterized in different biological tissues [35–39], but were not included in this research for the following reasons: In our

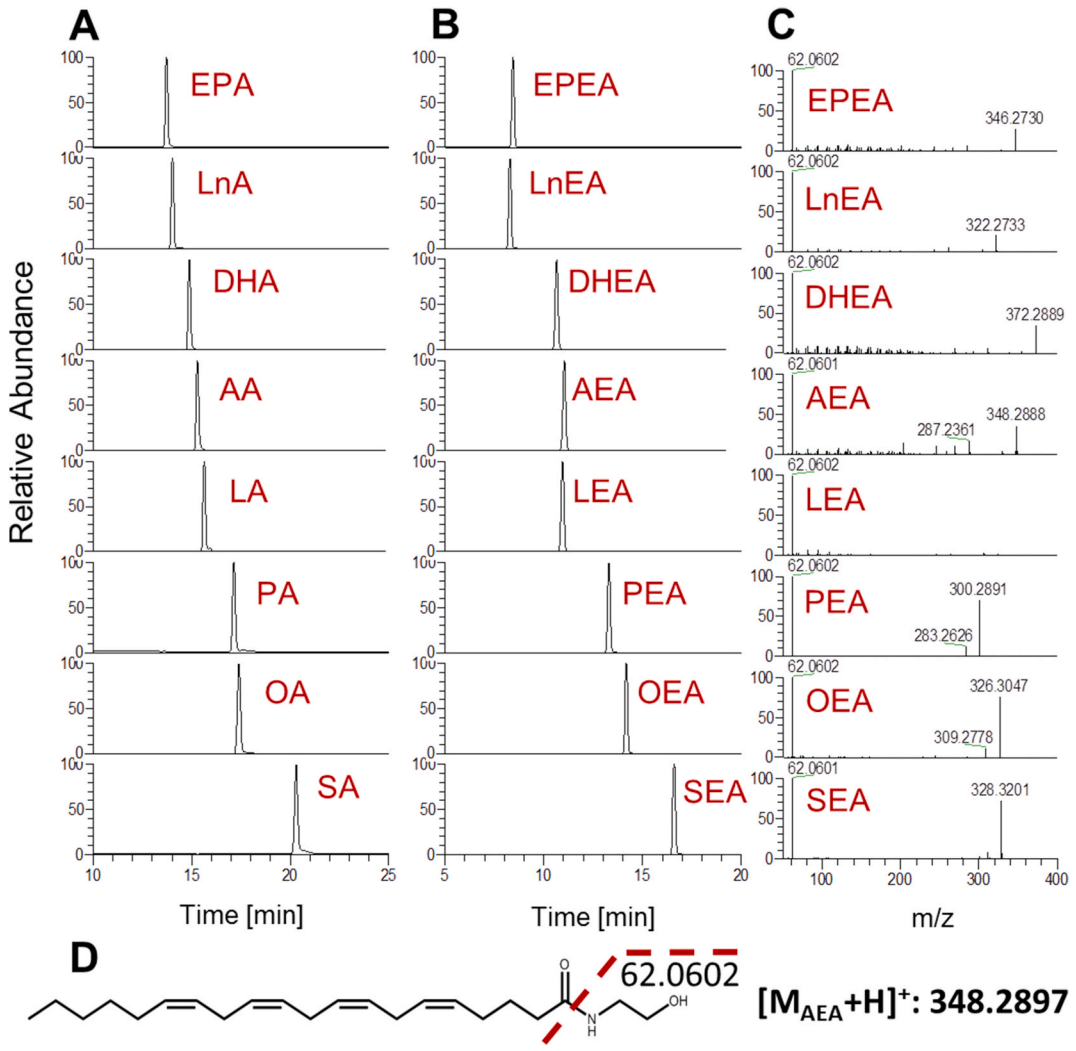

Fig. 3. Identification of fatty lipids by LC/HRMS/MS. Chromatographic elution of (**A**) FAs and (**B**) N-EAs from the UHPLC column. The relative order of elution for the same FA derivative is constant. (**C**) MS/MS spectra of N-EAs, with the corresponding $[M+H]^+$ accurate mass for each compound. As shown, all N-EA derivatives show the fragment with *m/z* of 62.0601, corresponding with the loss of the ethanolamine head group, as presented for (**D**) AEA.

method, N-acyl-dopamines and N-acyl-serotonins were found to degrade during the sample preparation procedure; when spiked into water, their concentrations decreased to approximately 80% of the initial concentration within 24 h. N-acyl taurines did not meet the requirements set for the method validation and were therefore excluded from this method. Derivatives of the cyclooxygenase-2 (COX-2), 12- and 15-lipoxygenases (12- and 15-LOX, respectively), and the CYP enzymes were successfully identified and extracted by the same method. However, biological samples contained noticeable matrix compounds with the same accurate masses as the oxygenated derivatives, and we therefore were not able to accurately quantify them in full MS^1 mode. This limitation could be overcome by a second injection of the same extracted samples to the instrument in PRM mode, using the optimized LC/HRMS transitions and RTs of several AA COX-2, 12- and 15-LOX derivatives, and AA, EPA and DHA derivatives of the CYP enzymes listed in Table S8.

Semi-quantification of additional identified cannabinoids without analytical standards, was performed according to the standard curve of a compound from the same lipid family (Table S9). These are approximated concentrations and should be referred to as such. However, semi-quantitative concentrations can still be compared to find significant differences between treatments in differential analyses, as is accepted in lipidomic studies.

3.3. eCB tone in central and peripheral tissues of mice

The developed method was first applied to study eCB concentrations in central and peripheral tissues of naïve mice (eCB tone). Since the eCBS plays different roles in the central nervous system (CNS) and in peripheral tissues [15,40–42], and cannabinoid receptors and metabolizing enzymes are differentially distributed throughout the body, in order to maintain specific functions depending on the tissue [15,30,34,43–47], we expected that the eCB concentrations would also vary between tissues. In Fig. 4, we show a differential analysis of average eCB concentrations in the brains, colons, livers and spleens of six healthy, 8–10 week old, male mice.

As shown, the levels of different analytes in the same tissue vary by over four orders of magnitude. Additionally, the concentrations of particular analytes vary in different tissues. Several lipid families were exclusively or considerably more highly expressed (>50%) in the brain compared to the other tissues, including N-EAs, N-acyl-serines and N-acyl gamma aminobutyric acids. Most N-acyl-amides and N-acyl-leucines had considerably higher contents in the colon compared to the other tissues.

Interestingly, when comparing the same compounds according to the FA tail (Fig. S3), it can be observed that the highest concentrations of most AA and DHA derivatives appeared in the brain. Polyunsaturated

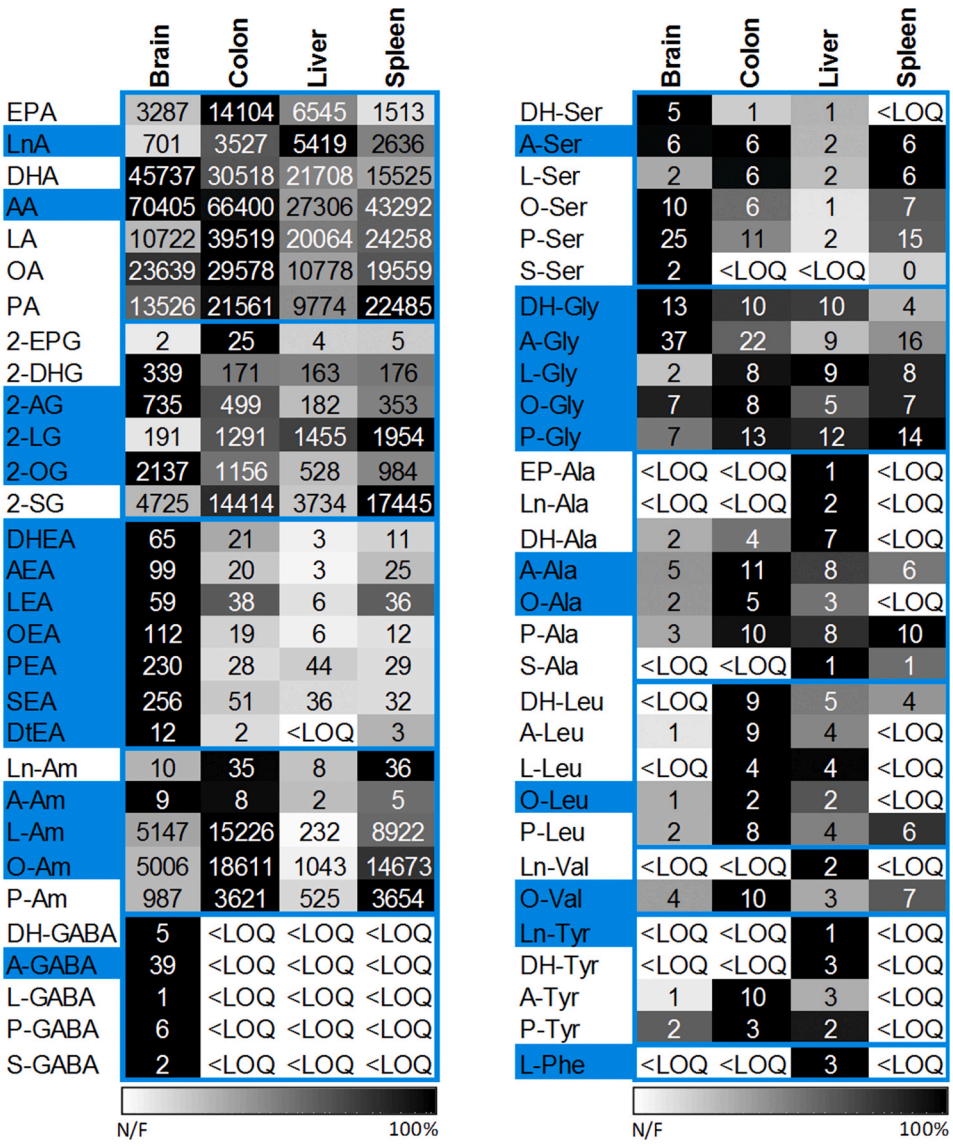

Fig. 4. Differential concentrations of eCBs in mouse tissues. Compounds are arranged by lipid class. The LC/HRMS concentrations of each compound were color coded in relation to the maximum value for each compound. Absolute values are in ng g^{-1} of tissue (n = 6). The names of compounds quantified according to analytical standards are marked in blue. Other compounds were semi-quantified according to the available analytical standard from the same lipid family, as detailed in Table S9. Only compounds that had concentrations above 1 ng g^{-1} in any of the tissues are presented. LOQ, limit of quantification. (For interpretation of the references to color in this figure legend, the reader is referred to the Web version of this article.)

fatty acids (PUFAs) including AA, DHA, EPA, LnA, and several of their mediators, have been found to be of clinical importance. AA, DHA and their mediators, including eCBs and oxylipins, have been found to regulate several processes within the brain, such as neurotransmission, cell survival and neuroinflammation [48]. The contents and signaling of several of these derivatives have been found to be altered in various neurological disorders [49].

3.4. *Differential modulation of eCB levels in the serum and brains of mice following treatment with different Cannabis chemovars*

In recent years, CBD-rich, oil-based *Cannabis* extracts have been introduced into the clinical setting for reducing seizures in children suffering from epilepsy and other indications [50]. However, although CBD is always the major phytocannabinoid component of decarboxylated *Cannabis* extracts derived from different CBD-rich *Cannabis* chemovars, it is plausible that other low level phytocannabinoids may also contribute to the anti-convulsant effects of *Cannabis* treatment, as recently suggested by our group [10]. In order to investigate this assumption for proof of concept, we challenged mice with either saline (control) or one of three CBD-rich extracts (CAN1-CAN3). These extracts had equally-high CBD levels (50% w/w), but varying concentrations of other minor phytocannabinoids (Fig. S4). Mice that were 30 min post-injection were sacrificed and both their serum and four sections of their brain (cortex, cerebellum, hippocampus and hypothalamus) were collected, extracted and analyzed using our LC/HRMS method.

In line with the observed differences in phytocannabinoid contents of the three extracts (Fig. S4), substantial phytocannabinoid variances were also detected between CAN1-CAN3 in the cortex of the challenged mice (Fig. 5A, the semi-quantitative absolute concentrations appear in Fig. S5). Several of the observed differences were statistically significant as shown for selected major phytocannabinoids (Fig. 5B). Phytocannabinoids in other brain parts, including the cerebellum, hippocampus and hypothalamus appear in Fig. S6A–S6C, respectively. For any particular extract, similar phytocannabinoid profiles were observed in all brain sections, and this profile varied in the serum, especially for CAN1 (Fig. 5B and Fig. S6A–S6C versus Fig. 5C, respectively). Suspecting that the observed differences in phytocannabinoid profiles may be due to phytocannabinoid metabolism, we also analyzed the concentrations of the putatively identified CBD metabolites in the different brain sections and in serum, as shown in the heatmap presented in Fig. 5D. The CBD metabolite names are listed in Fig. 2C. In order to compare the different metabolites, average concentrations were normalized against OH-CBD2 (C2) in each brain part or serum, and color coded by their values

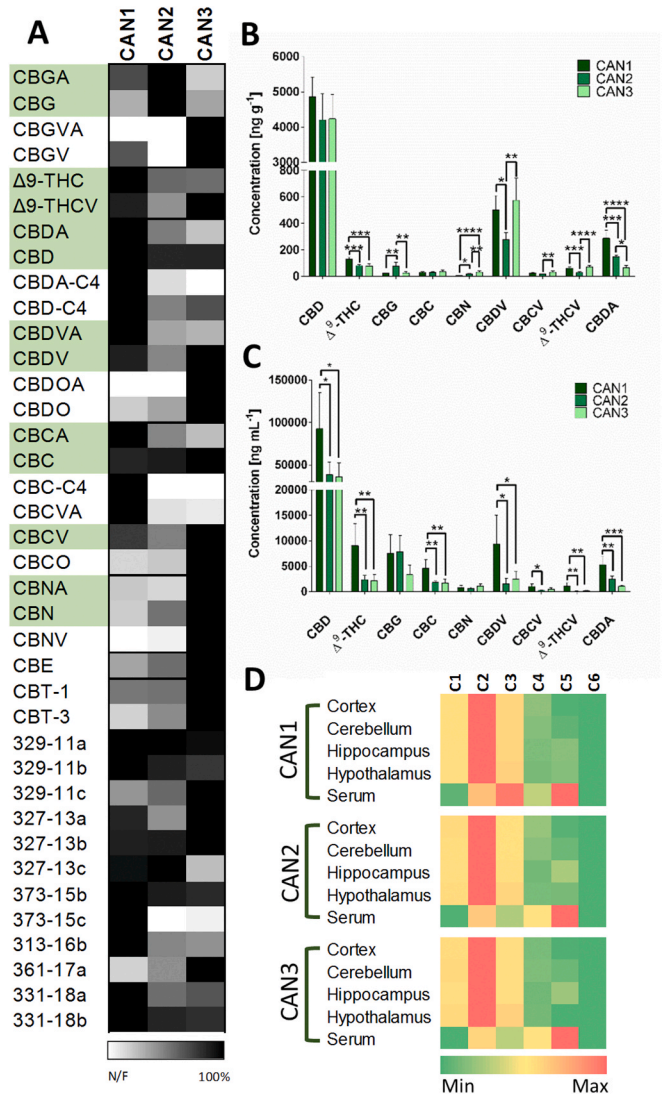

Fig. 5. Comparison of phytocannabinoid and major CBD metabolites concentrations in the cortex and serum of mice following *Cannabis* challenge. (**A**) Differential analysis of comprehensive phytocannabinoid concentrations in the cortex of mice challenged with three CBD-rich *Cannabis* extracts (CAN1-CAN3), sacrificed 30 min post injection. Only phytocannabinoids identified in at least one of the extracts appear in this analysis. The LC/HRMS concentrations of each compound were color coded in relation to the maximum value for each compound. The compounds with analytical standards are marked in green. Comparison of selected major phytocannabinoid concentrations in the (**B**) cortex and (**C**) serum of the challenged mice show significant differences between CAN1-CAN3. One-way ANOVA was used to determine statistical significance of five samples. P-values were corrected for multiple testing using the Tukey HSD post hoc test (*$p < 0.05$, **$p < 0.01$, ***$p < 0.001$, ****$p < 0.0001$). (**D**) Comparative average concentrations of the CBD metabolites in different brain sections and serum following *Cannabis* challenge. Average concentrations for each brain section or serum were normalized against C2. Concentrations were color coded from the minimum to the maximum values for each sample. (For interpretation of the references to color in this figure legend, the reader is referred to the Web version of this article.)

(Fig. 5D).

All the CBD metabolites in the brain exhibited very similar normalized values regardless of the brain section and *Cannabis* extract (hydroxylated CBD metabolites, and especially OH-CBD2, are most highly expressed in relation to the other metabolites), consistent with the similar CBD concentrations observed in all the brain parts. Serum concentrations, again showed different metabolite profiles compared to the brain, with the highest normalized concentration being of CBD-glucuronide (C5). Normalized concentrations of hydroxylated CBD metabolites were much lower in the serum compared to the brain. This is probably due to the CYP enzymes in the brain which have been found to metabolize phytocannabinoids [14]. The results also identify differences between brain and peripheral CBD metabolism. CAN1 has a different serum metabolite profile compared to the other *Cannabis* extracts [especially higher relative concentrations of OH-CBD3 (C3)]. This may be due to the differences in other-than CBD phytocannabinoids, as previously suggested for the altered pharmacokinetics of Δ^9-THC in the presence of CBD [51].

Concentrations of major N-EAs, MAGs and N-acyl glycines (N-Glys) in the mouse cortex appear in Fig. 6A–C, and for the cerebellum, hippocampus and hypothalamus in Fig. S7A–S7C, S7D-S7F and S7G-S7I, respectively. These groups of compounds have been suggested to be involved in the modulation of different physiological behaviors and/or pathological conditions in the brain [15,18,23,52,53]. Serum concentrations of N-EAs and MAGs appear in Fig. 6D and E, respectively. Concentrations of N-Glys in the serum were below the LOQ for most compounds. Annotated parts of the brain appear in Fig. 6F. All the compounds in this figure were quantified according to analytical standards. Unlike with the phytocannabinoids, basal concentrations of eCBs change in relation to the lipid family and brain part. According to this figure, a *Cannabis* challenge in the specified concentration and time point, significantly decreased the N-EA contents in the cortex and hippocampus compared to the controls (Fig. 6A and S7D, respectively). Interestingly, significant differences were also observed in several N-EAs in the cortex between CAN1 and CAN3 (Fig. 6A), suggesting an effect caused by other-than CBD phytocannabinoids (Fig. 5A). Several N-Glys in the cortex and cerebellum also showed significant reductions in eCB contents compared to the control group as a result of *Cannabis* challenge (Fig. 6C and S7C, respectively).

In order to test the hypotheses for the involvement of the eCBS in pathological or physiological conditions, many studies today analyze the contents of circulating eCBs. Phytocannabinoids and their metabolites are also frequently analyzed in the circulation in the context of *Cannabis* treatment, in order to study their pharmacokinetics, bioavailability in relation to specific formulations and modes of consumption, as well as their dose-response effects. This is mainly due to the fact that blood is relatively easy to sample, which is an important consideration, especially in human studies. However, circulating eCBs often do not represent local disturbances to the eCB tone as observed in specific tissues [34]. This is also the case for *Cannabis* treatment as shown in Fig. 6 and S7, where phytocannabinoids were found to exert different effects on eCB concentrations in the peripheral and central systems. Moreover, peripheral phytocannabinoid metabolism was found to lead to somewhat different profiles of phytocannabinoids and their metabolites, compared to the brain (Fig. 5 and S6). This emphasizes the importance of analyzing whole cannabinoids in the tissue of target in order to precisely evaluate the efficacy of the *Cannabis* treatment and elucidate mechanisms of action.

The observed modulation of eCB concentrations as a result of *Cannabis* challenge (Fig. 6A–C and S7) was found to differ between brain sections with different functions. This is consistent with a recent study that investigated the effect of acute Δ^9-THC on the developing brain, and concluded that Δ^9-THC changes the brain lipidome and transcriptome differentially in the adolescent and the adult mouse [30]. In this study, we further demonstrate for the first time, that different *Cannabis* extracts with equal amounts of CBD but different phytocannabinoid profiles (Fig. S4), led to differential effects on the eCB metabolome. We feel it is important to note that these phytocannabinoid contents and effects are time- and concentration-dependent. In order to analyze the exact effect of phytocannabinoids on the eCB metabolome, it is important to determine the dosing effect of a specific extract, and to analyze several time points. It should also be noted that the observed variations in eCB mediator levels could be due to several other factors, including other

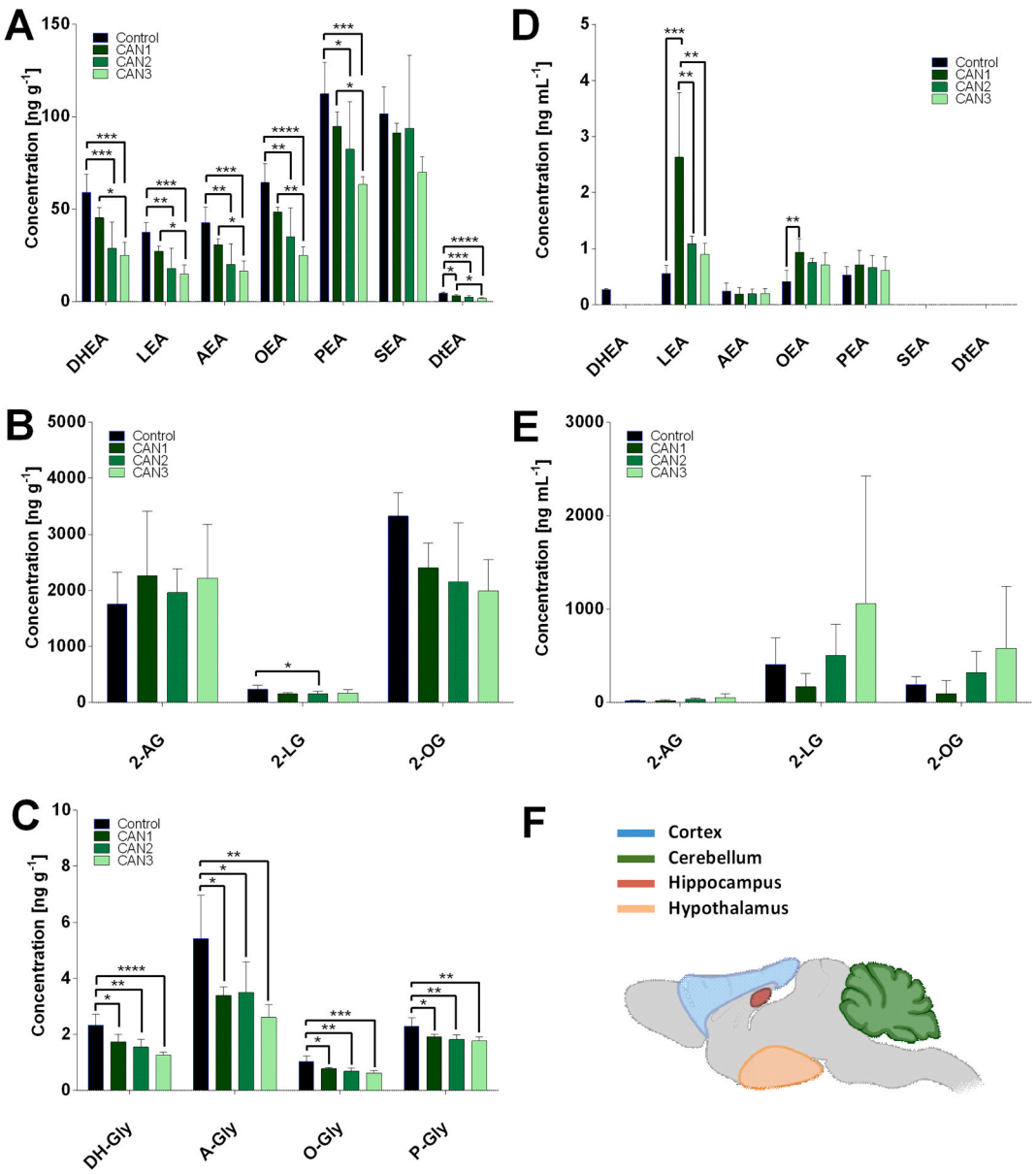

Fig. 6. Modulation of the endocannabinoid metabolome in different brain sections and serum following *Cannabis* challenge. Concentrations of selected major (**A**) N-EAs, (**B**) MAGs and (**C**) N-Glys in the cortex; and (**D**) N-EAs and (**E**) MAGs in the serum of mice, challenged with either saline (control) or one of the three CBD-rich *Cannabis* extracts (CAN1-CAN3). One-way ANOVA was used to determine statistical significance of five samples. P-values were corrected for multiple testing using the Tukey HSD post hoc test (*$p < 0.05$, **$p < 0.01$, ***$p < 0.001$, ****$p < 0.0001$). The excised brain parts appear in (**F**).

non-phytocannabinoid components in the extracts, or the presence of CBD itself that is accompanied by other molecules, which may alter its capability of eCB degradation or cellular reuptake, as suggested by De Petrocellis et al. [54]. In order to suggest a cause-effect relationship between the administration of different extracts and their effects on the eCBS, a more detailed study including dose-response effects and mechanistic considerations, should be employed. However, this was beyond the scope of the current study and remains for future research.

4. Conclusions

In this study, we describe the development and validation of an analytical approach, termed "cannabinoidomics." The method's fundamental principles and main strengths include: (a) the establishment of a novel cannabinoidomic library based on the compounds identified in this study, including 57 phytocannabinoids, 15 Δ^9-THC and CBD metabolites, and 78 eCBs; (b) the development of single extraction and LC/HRMS methods for simultaneous extraction and comprehensive profiling of all the cannabinoids in the cannabinoidomic library, and from numerous biological matrices; and (c) the validation of the developed method for the compounds with analytical standards.

For proof of concept, we validated this method by analyzing the serum and brains of mice challenged with three different CBD-rich extracts. Our results demonstrate that different *Cannabis* extracts lead to varied effects on eCB concentrations, and on the CBD metabolite profile in the peripheral and central systems. These could be due to the content of the minor phytocannabinoid or non-cannabinoid contents in the different extracts, and should be further researched by applying the developed approach. This type of modulation of the eCBS has been suggested as an emerging target of pharmacotherapy. It is important, therefore, that biological and pharmaceutical preclinical and human studies that involve the eCBS, will derive accurate and comprehensive measurements of whole cannabinoids in biological matrices. We envision that the application of the developed approach in these studies will

enable further elucidation of the involvement of the eCBS in various physiological and pathological conditions, in order to study the efficacy and safety of *Cannabis* treatment on these conditions, and to ultimately develop new *Cannabis*-based therapeutics.

Authorship contribution statement

Paula Berman: Conceptualization, Investigation, Methodology, Validation, Visualization, Writing - original draft. Liron Sulimani: Conceptualization, Investigation, Methodology, Validation, Visualization, Writing - review & editing. Anat Gelfand: Investigation. Keren Amsalem: Investigation. Gil M. Lewitus: Conceptualization, Writing - review & editing, Supervision. David Meiri: Conceptualization, Resources, Writing - review & editing, Funding acquisition, Supervision.

Declaration of competing interest

The authors declare that they have no known competing financial interests or personal relationships that could have appeared to influence the work reported in this paper.

Acknowledgments

We thank the Evelyn Gruss Lipper Charitable Foundation and the Israeli Ministry of Agriculture and Rural Development, for their financial support of this work. The authors would like to thank Cannasoul Analytics for the help in method development; Dr. Ailie Marx and Dr. Roni Enten Vissoker for the critical comments and editing of the manuscript; Dr. Dafna Antes for the graphical design of the graphical abstract; and Mr. Ohad Guberman for the extraction and sample preparation of the *Cannabis* extracts.

Appendix A. Supplementary data

Supplementary data to this article can be found online at https://doi.org/10.1016/j.talanta.2020.121336.

References

[1] P. Pacher, G. Kunos, Modulating the endocannabinoid system in human health and disease–successes and failures, FEBS J. 280 (2013) 1918–1943.
[2] V. Di Marzo, F. Piscitelli, The endocannabinoid system and its modulation by phytocannabinoids, Neurotherapeutics 12 (2015) 692–698.
[3] J. Hwang, C. Adamson, D. Butler, D.R. Janero, A. Makriyannis, B.A. Bahr, Enhancement of endocannabinoid signaling by fatty acid amide hydrolase inhibition: a neuroprotective therapeutic modality, Life Sci. 86 (2010) 615–623.
[4] V.K. Vemuri, A. Makriyannis, Medicinal chemistry of cannabinoids, Clin. Pharmacol. Ther. 97 (2015) 553–558.
[5] R.G. Pertwee, A.C. Howlett, M.E. Abood, S.P. Alexander, V. Di Marzo, M. R. Elphick, P.J. Greasley, H.S. Hansen, G. Kunos, K. Mackie, R. Mechoulam, International union of basic and clinical pharmacology. LXXIX. Cannabinoid receptors and their ligands: beyond CB1 and CB2, Pharmacol. Rev. 62 (2010) 588–631.
[6] E. Leishman, H.B. Bradshaw, N-acyl amides: ubiquitous endogenous cannabimimetic lipids that are in the right place at the right time, in: V. Di Marzo, J. Wang (Eds.), The Endocannabinoidome, Academic Press, 2015, pp. 33–48.
[7] O. Aizpurua-Olaizola, I. Elezgarai, I. Rico-Barrio, I. Zarandona, N. Etxebarria, A. Usobiaga, Targeting the endocannabinoid system: future therapeutic strategies, Drug Discov. Today 22 (2017) 105–110.
[8] M. ElSohly, W. Gul, Constituents of *Cannabis sativa*, in: R.G. Pertwee (Ed.), Handbook of Cannabis, Oxford University Press, New York, 2014, pp. 3–22.
[9] L.O. Hanuś, S.M. Meyer, E. Muñoz, O. Taglialatela-Scafati, G. Appendino, Phytocannabinoids: a unified critical inventory, Nat. Prod. Rep. 33 (2016) 1357–1392.
[10] P. Berman, K. Futoran, G.M. Lewitus, D. Mukha, M. Benami, T. Shlomi, D. Meiri, A new ESI-LC/MS approach for comprehensive metabolic profiling of phytocannabinoids in *Cannabis*, Sci. Rep. 8 (2018) 14280.
[11] R. Mechoulam, Marihuana Chemistry, Science 168 (1970) 1159–1166.
[12] F. Grotenhermen, Pharmacokinetics and pharmacodynamics of cannabinoids, Clin. Pharmacokinet. 42 (2003) 327–360.
[13] M.A. Huestis, Pharmacokinetics and metabolism of the plant cannabinoids, Δ^9-tetrahydrocannibinol, cannabidiol and cannabinol, in: R.G. Pertwee (Ed.), Cannabinoids, Handbook of Experimental Pharmacology, vol. 168, Springer, Berlin, 2005, pp. 657–690.
[14] D.J. Harvey, N.K. Brown, Comparative in vitro metabolism of the cannabinoids, Pharmacol. Biochem. Behav. 40 (1991) 533–540.
[15] A. Ligresti, L. De Petrocellis, V. Di Marzo, From phytocannabinoids to cannabinoid receptors and endocannabinoids: pleiotropic physiological and pathological roles through complex pharmacology, Physiol. Rev. 96 (2016) 1593–1659.
[16] S.E. Turner, C.M. Williams, L. Iversen, B.J. Whalley, Molecular pharmacology of phytocannabinoids, in: A.D. Kinghorn, H. Falk, S. Gibbons, J. Kobayashi (Eds.), Phytocannabinoids, Springer International Publishing, Switzerland, 2017, pp. 61–101.
[17] P. Morales, D.P. Hurst, P.H. Reggio, Molecular targets of the phytocannabinoids: a complex picture, in: A.D. Kinghorn, H. Falk, S. Gibbons, J. Kobayashi (Eds.), Phytocannabinoids, Springer International Publishing, Switzerland, 2017, pp. 103–131.
[18] J. Williams, J. Wood, L. Pandarinathan, D.A. Karanian, B.A. Bahr, P. Vouros, A. Makriyannis, Quantitative method for the profiling of the endocannabinoid metabolome by LC-atmospheric pressure chemical ionization-MS, Anal. Chem. 79 (2007) 5582–5593.
[19] T. Bisogno, F. Piscitelli, V. Di Marzo, Lipidomic methodologies applicable to the study of endocannabinoids and related compounds: Endocannabinoidomics, Eur. J. Lipid Sci. Technol. 111 (2009) 53–63. .
[20] B. Tan, D.K. O'Dell, Y.W. Yu, M.F. Monn, S. Burstein, J.M. Walker, Identification of endogenous acyl amino acids based on a targeted lipidomics approach, J. Lipid Res. 51 (2010) 112–119.
[21] F. Piscitelli, Endocannabinoidomics: "Omics" approaches applied to endocannabinoids and endocannabinoid-like mediators, in: V. Di Marzo, J. Wang (Eds.), The Endocannabinoidome, Academic Press, 2015, pp. 137–152.
[22] F. Piscitelli, H.B. Bradshaw, Endocannabinoid analytical methodologies: techniques that drive discoveries that drive techniques, in: D. Kendall, S.P. H. Alexander (Eds.), Advances in Pharmacology 80, Academic Press, 2017, pp. 1–30.
[23] S.H. Burstein, N-Acyl amino acids (Elmiric Acids): endogenous signaling molecules with therapeutic potential, Mol. Pharmacol. 93 (2018) 228–238.
[24] W.H. Abd-Elsalam, M.A. Alsherbiny, J. Kung, D.W. Pate, R. Löbenberg, LC–MS/MS quantitation of phytocannabinoids and their metabolites in biological matrices, Talanta 204 (2019) 846–867.
[25] J. Jung, M.R. Meyer, H.H. Maurer, C. Neusüß, W. Weinmann, V. Auwärter, Studies on the metabolism of the Δ^9-tetrahydrocannabinol precursor Δ^9-tetrahydrocannabinolic acid A (Δ^9-THCA-A) in rat using LC-MS/MS, LC-QTOF MS and GC-MS techniques, J. Mass Spectrom. 44 (2009) 1423–1433.
[26] S. Deiana, A. Watanabe, Y. Yamasaki, N. Amada, M. Arthur, S. Fleming, H. Woodcock, P. Dorward, B. Pigliacampo, S. Close, B. Platt, Plasma and brain pharmacokinetic profile of cannabidiol (CBD), cannabidivarine (CBDV), Δ^9-tetrahydrocannabivarin (THCV) and cannabigerol (CBG) in rats and mice following oral and intraperitoneal administration and CBD action on obsessive–compulsive behavior, Psychopharmacology 219 (2012) 859–873.
[27] K.B. Scheidweiler, M.N. Newmeyer, A.J. Barnes, M.A. Huestis, Quantification of cannabinoids and their free and glucuronide metabolites in whole blood by disposable pipette extraction and liquid chromatography-tandem mass spectrometry, J. Chromatogr. A 1453 (2016) 34–42.
[28] F. Piscitelli, E. Pagano, A. Lauritano, A.A. Izzo, V. Di Marzo, Development of a rapid LC-MS/MS method for the quantification of cannabidiol, cannabidivarin, Δ^9-tetrahydrocannabivarin, and cannabigerol in mouse peripheral tissues, Anal. Chem. 89 (2017) 4749–4755.
[29] L. Baram, E. Peled, P. Berman, B. Yellin, E. Besser, M. Benami, I. Louria-Hayon, G. M. Lewitus, D. Meiri, The heterogeneity and complexity of *Cannabis* extracts as antitumor agents, Oncotarget 10 (2019) 4091.
[30] E. Leishman, M. Murphy, K. Mackie, H.B. Bradshaw, Δ^9-Tetrahydrocannabinol changes the brain lipidome and transcriptome differentially in the adolescent and the adult, Biochim. Biophys. Acta Mol. Cell Biol. Lipids 1863 (2018) 479–492.
[31] A.A. Zoerner, F.M. Gutzki, S. Batkai, M. May, C. Rakers, S. Engeli, J. Jordan, D. Tsikas, Quantification of endocannabinoids in biological systems by chromatography and mass spectrometry: a comprehensive review from an analytical and biological perspective, Biochim. Biophys. Acta Mol. Cell Biol. Lipids 1811 (2011) 706–723.
[32] M.G. Balvers, H.M. Wortelboer, R.F. Witkamp, K.C. Verhoeckx, Liquid chromatography–tandem mass spectrometry analysis of free and esterified fatty acid N-acyl ethanolamines in plasma and blood cells, Anal. Biochem. 434 (2013) 275–283.
[33] M. Qi, M. Morena, H.A. Vecchiarelli, M.N. Hill, D.C. Schriemer, A robust capillary liquid chromatography/tandem mass spectrometry method for quantitation of neuromodulatory endocannabinoids, Rapid Commun. Mass Spectrom. 29 (2015) 1889–1897.
[34] C.J. Hillard, Circulating endocannabinoids: from whence do they come and where are they going? Neuropsychopharmacology 43 (2018) 155.
[35] C.J. Chu, S.M. Huang, L. De Petrocellis, T. Bisogno, S.A. Ewing, J.D. Miller, R. E. Zipkin, N. Daddario, G. Appendino, V. Di Marzo, J.M. Walker, N-Oleoyldopamine, A novel endogenous capsaicin-like lipid that produces hyperalgesia, J. Biol. Chem. 278 (2003) 13633–13639.
[36] L. De Petrocellis, C.J. Chu, A.S. Moriello, J.C. Kellner, J.M. Walker, V. Di Marzo, Actions of two naturally occurring saturated N-acyldopamines on transient receptor potential vanilloid 1 (TRPV1) channels, Br. J. Pharmacol. 143 (2004) 251–256.
[37] K.C.M. Verhoeckx, T. Voortman, M.G.J. Balvers, H.F.J. Hendriks, H.M. Wortelboer, R.F. Witkam, Presence, formation and putative biological activities of N-acyl serotonins, a novel class of fatty-acid derived mediators, in the intestinal tract, Biochim. Biophys. Acta 1811 (2011) 578–586.

[38] A. Saghatelian, S.A. Trauger, E.J. Want, E.G. Hawkins, G. Siuzdak, B.F. Cravatt, Assignment of endogenous substrates to enzymes by global metabolite profiling, Biochemistry 43 (2004), 14339–14332.
[39] A. Saghatelian, M.K. McKinney, M. Bandell, A. Patapoutian, B.F. Cravatt, A FAAH-regulated class of N-acyl taurines that activates TRP ion channels, Biochemistry 45 (2006) 9007–9015.
[40] I. Matias, T. Bisogno, V. Di Marzo, Endogenous cannabinoids in the brain and peripheral tissues: regulation of their levels and control of food intake, Int. J. Obes. 30 (2006). S7–S12.
[41] A. Ligresti, S. Petrosino, V. Di Marzo, From endocannabinoid profiling to 'endocannabinoid therapeutics', Curr. Opin. Chem. Biol. 13 (2009) 321–331.
[42] S. Hirsch, J. Tam, Cannabis, From a plant that modulates feeding behaviors toward developing selective inhibitors of the peripheral endocannabinoid system for the treatment of obesity and metabolic syndrome, Toxins 11 (2019) 275.
[43] S. Galiègue, S. Mary, J. Marchand, D. Dussossoy, D. Carrière, P. Carayon, M. Bouaboula, D. Shire, G. Le Fur, P. Casellas, Expression of central and peripheral cannabinoid receptors in human immune tissues and leukocyte subpopulations, Eur. J. Biochem. 232 (1995) 54–61.
[44] A.B. Lynn, M. Herkenham, Localization of cannabinoid receptors and nonsaturable high-density cannabinoid binding sites in peripheral tissues of the rat: implications for receptor-mediated immune modulation by cannabinoids, J. Pharmacol. Exp. Therapeut. 268 (1994) 1612–1623.
[45] R.G. Pertwee, Pharmacology of cannabinoid CB1 and CB2 receptors, Pharmacol. Ther. 74 (1997) 129–180.
[46] R.G. Pertwee, Evidence for the presence of CB1 cannabinoid receptors on peripheral neurones and for the existence of neuronal non-CB1 cannabinoid receptors, Life Sci. 65 (1999) 597–605.
[47] J.Z. Long, D.K. Nomura, B.F. Cravatt, Characterization of monoacylglycerol lipase inhibition reveals differences in central and peripheral endocannabinoid metabolism, Chem. Biol. 16 (2009) 744–753.
[48] R.P. Bazinet, S. Layé, Polyunsaturated fatty acids and their metabolites in brain function and disease, Nat. Rev. Neurosci. 15 (2014) 771–785.
[49] S.G. Snowden, A.A. Ebshiana, A. Hye, Y. An, O. Pletnikova, R. O'Brien, J. Troncoso, C. Legido-Quigley, M. Thambisetty, Association between fatty acid metabolism in the brain and Alzheimer disease neuropathology and cognitive performance: a nontargeted metabolomic study, PLoS Med. 14 (2017), e1002266.
[50] N.A. Jones, A.J. Hill, I. Smith, S.A. Bevan, C.M. Williams, B.J. Whalley, G. J. Stephens, Cannabidiol displays antiepileptiform and antiseizure properties *in vitro* and *in vivo*, J. Pharmacol. Exp. Therapeut. 332 (2010) 569–577.
[51] C. Klein, E. Karanges, A. Spiro, A. Wong, J. Spencer, T. Huynh, N. Gunasekaran, T. Karl, L.E. Long, X.F. Huang, K. Liu, Cannabidiol potentiates Δ^9-tetrahydrocannabinol (THC) behavioural effects and alters THC pharmacokinetics during acute and chronic treatment in adolescent rats, Psychopharmacology 218 (2011) 443–457.
[52] N. Murataeva, A. Dhopeshwarkar, D. Yin, J. Mitjavila, H. Bradshaw, A. Straiker, K. Mackie, Where's my entourage? The curious case of 2-oleoylglycerol, 2-linolenoylglycerol, and 2-palmitoylglycerol, Pharmacol. Res. 110 (2016) 173–180.
[53] G. Donvito, F. Piscitelli, P. Muldoon, A. Jackson, R.M. Vitale, E. D'Aniello, C. Giordano, B.M. Ignatowska-Jankowska, M.A. Mustafa, F. Guida, G.N. Petrie, N-Oleoyl-glycine reduces nicotine reward and withdrawal in mice, Neuropharmacology 148 (2019) 320–331.
[54] L. De Petrocellis, A. Ligresti, A.S. Moriello, M. Allarà, T. Bisogno, S. Petrosino, C. G. Stott, V. Di Marzo, Effects of cannabinoids and cannabinoid-enriched Cannabis extracts on TRP channels and endocannabinoid metabolic enzymes, Br. J. Pharmacol. 163 (2011) 1479–1494.